

Excitation of S_{11} resonances in pion scattering and pion photoproduction on the proton

Guan-Yeu Chen, Sabit Kamalov* and Shin Nan Yang

Department of Physics, National Taiwan University, Taipei, Taiwan 10764, Republic of China

Dieter Drechsel and Lothar Tiator

Institut für Kernphysik, Universität Mainz, 55099 Mainz, Germany

(May 21, 2019)

A self-consistent analysis of pion scattering and pion photoproduction within a coupled channels dynamical model is presented. The results indicate the existence of a third and a fourth S_{11} resonance with the masses 1803 ± 7 and 2117 ± 64 MeV. In the case of pion photoproduction, we obtain background contributions to the imaginary part of the S -wave multipole which differ considerably from the result based on the K-matrix approximation. Within the dynamical model these background contributions become large and negative in the region of the $S_{11}(1535)$ resonance. Due to this fact much larger resonance contributions are required in order to explain the results of the recent multipole analyses. For the first $S_{11}(1535)$ resonance we obtain as a value of the electromagnetic helicity amplitude: $A_{1/2} = 72 \pm 2 \times 10^{-3} \text{ GeV}^{-1/2}$. Similar values can be derived from eta photoproduction if one takes the same total width ($\Gamma_R = 95 \pm 5$ MeV) as in pion scattering and pion photoproduction.

Hadron spectroscopy has always played an important role in unravelling the underlying quark dynamics. For example, the pattern of similarity between the eight baryons and the eight pseudoscalar mesons led to the epochal discovery of SU(3) symmetry.

There are 44 nonstrange baryon states listed in the 2000 publication of the Particle Data Group [1], 22 each in $T = \frac{1}{2}$ and $T = \frac{3}{2}$ channels, respectively. Among them, 18 are rated four-star and 6 rated three-star. The rest are weakly excited states with at most fair evidence of existence. Even though the existence of the four-star baryon resonances are certain, some very large discrepancies exist in their properties as obtained from different analyses. One example is the extracted width of the four-star $S_{11}(1535)$ state given as 66 MeV [2], 120 ± 20 MeV [3], 151 ± 27 MeV [4], $151 - 198$ MeV [5], and 270 ± 50 MeV [6]. The differences between different analyses arise mostly from the data set included in the analysis, or the separation of background and resonance contributions, among others. This model dependence in the extraction of the resonance properties has made it difficult to test the predictions of theoretical models with existing data.

At present most of the resonance properties are extracted from πN scattering and pion photoproduction. We have recently developed a meson-exchange (MEX) model [7] for pion-nucleon scattering which gives good agreement with the data up to 400 MeV pion lab energy. In addition, we have also constructed a dynamical model for pion electromagnetic production [8,9] which describes well the π^0 photo- and electro-production data near threshold [10] and most of the existing pion electromagnetic production data up to the second resonance region. In this paper, we extend our meson-exchange πN model in the S_{11} channel up to 2 GeV by explicitly introducing the known S_{11} resonances into the model. The resulting πN model in the S_{11} channel is then fed into the pion photoproduction model to analyze the existing pE_{0+} multipole. The S_{11} channel is of interest for several reasons. First of all, the first resonance $S_{11}(1535)$, which lies only 48 MeV above the ηN threshold, has a remarkably large ηN branching ratio. This necessitates to include the ηN channel into our MEX πN model. Secondly, the analyses based solely on pion photoproduction always underestimate the $A_{1/2}^p$ helicity amplitude of $S_{11}(1535)$ with a value around 60×10^{-3} $\text{GeV}^{-1/2}$, while extractions from the (γ, η) data give a value close to and above $100 \times 10^{-3} \text{ GeV}^{-1/2}$ [1]. Lastly, there have been suggestions [11,12] that there could exist a third S_{11} resonance lying in the neighborhood of 1800 – 1900 MeV, in addition to the well-known resonances at 1535 and 1650 MeV. A consistent analysis of both πN scattering and pion photoproduction reactions can shed new light on the issues mentioned above concerning helicity amplitudes and higher resonance as well as reduce the large uncertainties in the width obtained from previous analyses.

Our MEX πN model is obtained by using a three-dimensional reduction scheme of the Bethe-Salpeter equation for a model Lagrangian involving π , N , Δ , ρ , and σ fields. Details can be found in Ref. [7]. Here we only present the general scheme to extend the model to the case of coupled π , η and 2π channels, including in addition the couplings with baryon resonances in the S_{11} partial wave. To do this, we first enlarge the Hilbert space to include a bare S_{11} particle R which acquires a width by couplings with πN and ηN channels via the Lagrangian

$$\mathcal{L}_{\mathcal{I}} = ig_{\pi NR}^{(0)} \bar{R} \boldsymbol{\tau} N \cdot \boldsymbol{\pi} + ig_{\eta NR}^{(0)} \bar{R} N \eta + h.c., \quad (1)$$

where N, R, π , and η denote the field operators for the nucleon, bare R , pion and eta meson, respectively. Then the full t -matrix can be written as a system of coupled equations,

$$t_{ij}(E) = v_{ij}(E) + \sum_k v_{ik}(E) g_k(E) t_{ki}(E), \quad (2)$$

where i and j denote the π , or η channel and $E = W$ is the total center mass energy. Eq. (2) is a system of three dimensional coupled integral equations which is derived from the four dimensional Bethe-Salpeter equation using a three-dimensional reduction scheme with a corresponding relativistic propagator, g_k , for the free kN system ($k = \pi$, or η). In this paper, we employ the Cooper-Jennings reduction scheme [13].

The potential v_{ij} , in general, is a sum of non-resonant, v_{ij}^B , and bare resonance, v_{ij}^R , terms,

$$v_{ij}(E) = v_{ij}^B(E) + v_{ij}^R(E). \quad (3)$$

The non-resonant term $v_{\pi\pi}^B$ for the πN elastic channel contains contributions from the s - and u -channel, Born terms and t -channel contributions with ω , ρ , and σ exchange. In the present work the parameters in $v_{\pi\pi}^B$ are fixed from the analysis of the pion scattering phase shifts for the s - and p -waves at low energies ($W < 1300$ MeV). In channels involving η , $v_{\eta\eta}^B$ is taken to be zero since the ηNN coupling is very small [14]. The bare resonance contribution $v_{ij}^R(E)$ arises from the excitation and de-excitation of the resonance R via the interaction Lagrangian of Eq. (1).

Let us first consider the case with only one resonance contributing in the S_{11} channel in the energy region of interest, i.e., $W \leq 2$ GeV. The corresponding potential $v_{ij}^R(E)$ can then be symbolically expressed in the form of

$$v_{ij}^R(q, q'; E) = \frac{f_i(\tilde{\Lambda}_i, q; E) g_i^{(0)} g_j^{(0)} f_j(\tilde{\Lambda}_j, q'; E)}{E - M_R^{(0)} + i \frac{1}{2} \Gamma_{2\pi}^R(E)}, \quad (4)$$

where q and q' are the pion (or eta) momenta in the initial and final states, $g_{i(j)}^{(0)}$ and $M_R^{(0)}$ are the bare resonance vertex couplings and bare masses, respectively. In line with our previous πN model, we associate with each line of a particle α in the Feynman diagram a covariant form factor F_α of the form $[n_\alpha \Lambda_\alpha^4 / (n_\alpha \Lambda_\alpha^4 + (p_\alpha^2 - m_\alpha^2)^2)]^{n_\alpha}$, where p_α , m_α , and Λ_α are the four-momentum, mass, and cut-off parameter of particle α , respectively. Accordingly, f_i of Eq. (4), is a product of three F'_α 's, each one of them corresponding to one of the three legs associated with the considered vertex. Subsequently, f_i depends on three cut-off parameters, i.e., $\tilde{\Lambda}_\pi \equiv (\Lambda_N, \Lambda_R, \Lambda_\pi)$. We refer the readers to Refs. [7,15] for details and only mention that $n_\alpha = 10$ is used in the present work.

In Eq. (4) we have added a phenomenological term $\Gamma_{2\pi}^R(E)$ in the resonance propagator in order to take into account the decay of the resonance into the $\pi\pi N$ channel. Therefore, our resonance propagator is not purely "bare" but includes renormalization (or "dressing") effects due to the coupling with the $\pi\pi N$ channel. Using this prescription we assume that the additional non-resonant mechanisms of coupling with the $\pi\pi N$ channel are small. Following Refs. [16,17] we take $\Gamma_{2\pi}^R(E)$ as

$$\Gamma_{2\pi}^R(E) = \Gamma_{2\pi}^{0,R} \left(\frac{q_{2\pi}}{q_0} \right)^{2l+4} \left(\frac{X^2 + q_0^2}{X^2 + q_{2\pi}^2} \right)^{l+2}, \quad (5)$$

where $q_{2\pi}$ is the momentum of the compound (2π) system with mass $2m_\pi$ and $q_0 = q_{2\pi}$ at $E = M_R^{(0)}$. Note that this form takes account of the correct energy behavior of the phase space near the three-body threshold [17]. The parameter X is fixed at 500 MeV as suggested in Ref. [16]. The quantity $\Gamma_{2\pi}^{0,R}$ is associated with the 2π decay width at the resonance position. In general, it can be considered as a free parameter. However, its value is strongly correlated with the values of the unknown coupling constants $g_i^{(0)}$ (usually a small $g_i^{(0)}$ requires a large $\Gamma_{2\pi}^{0,R}$). Therefore, we will fix the value for $\Gamma_{2\pi}^{0,R}$ by use of recent knowledge about the decay modes of the resonances and their total Breit-Wigner widths [1].

Summarizing our parametrization of the potential v_{ij}^R in the case of coupled pion and eta channels, we would like to emphasize that, in general, one isolated resonance contains five free parameters, namely: the bare mass, $M_R^{(0)}$, the decay width $\Gamma_{2\pi}^0$, two bare coupling constants $g_i^{(0)}$ and $g_j^{(0)}$, and one cutoff parameter Λ_R . However, if the decay in the eta channel is strongly suppressed, e.g. in the case of $S_{11}(1650)$, the number of free parameters is reduced to four: $M_R^{(0)}$, $\Gamma_{2\pi}^{0,R}$, $g_{\pi NR}^{(0)}$, and Λ_R .

In the channel of interest, S_{11} , there are two well-known four-star resonance states, $S_{11}(1535)$ and $S_{11}(1650)$, and one one-star resonance, $S_{11}(2090)$. In the Hypercentral Constituent Quark Model [11] a third and a fourth S_{11}

resonance with energies 1860 and 2008 MeV were predicted. The generalization of our coupled channels model for multiple resonances with the same quantum numbers is straightforward, namely

$$v_{ij}^R(q, q'; E) = \sum_{n=1}^N v_{ij}^{R_n}(q, q'; E), \quad (6)$$

with additional parameters for the bare masses, widths, coupling constants and cut-off parameters for each resonance.

We first start with the analysis of $\text{Re } t_{\pi\pi}$ and $\text{Im } t_{\pi\pi}$ in the energy range $1100 < W < 1750$ MeV where the $S_{11}(1535)$ and $S_{11}(1650)$ resonances are very pronounced. The results of our best fit in this energy range with only these two resonances included are shown in Fig. 1 by the dotted curves. We are not able to improve our results in the $W > 1800$ MeV region without additional S_{11} resonances. Next we extend the energy range of the fitting up to $W = 2000$ MeV and add a third resonance with parameters for the first resonance fixed as obtained above. Our results for this case are shown by the dash-dotted curves, which correspond to a bare mass of the third S_{11} resonance $M_3^{(0)} = 1791$ MeV. We find that this value is very stable and changes only within 2% if the energy range is increased up to 2200 MeV. However, this does not remove the remaining discrepancy, in particular for the imaginary part at $W > 2000$ MeV. We find that the only way to improve the agreement with the data in this energy range is to introduce a fourth resonance. Our final results of the fitting ($\chi/120 = 4.56$) with four S_{11} resonances are shown by the solid lines in Fig. 1. The obtained value for the bare mass of the fourth S_{11} resonance is $M_4^{(0)} = 2160$ MeV. Note that in Fig. 1 the background contributions (dashed curves) are defined by the equation $\tilde{t}_{\pi\pi}^B(E) = v_{\pi\pi}^B(E) + v_{\pi\pi}^B(E) g(E) \tilde{t}_{\pi\pi}^B(E)$ (hereafter called the "nonresonant background", i.e., background with nonresonant rescattering).

Now let us turn to the more sophisticated part of the analysis, namely, the extraction of the physical (or "dressed") masses, partial widths and branching ratios of the resonances. As was pointed out in Ref. [18], the procedure is in general model dependent. This is mainly connected with the question how to separate background and resonance contributions in a well-defined way. The solution to this problem becomes more difficult with increasing number of the overlapping resonances in the same channel. Below we present our solution to this problem.

First, we will determine the physical mass using the following definition for the contribution of the n -th resonance R_n in the elastic pion scattering channel:

$$t_{\pi\pi}^{R_n}(E) = v_{\pi\pi}^{R_n}(E) + \sum_k v_{\pi k}^{R_n}(E) g_k(E) t_{k\pi}(E), \quad (7)$$

with $t_{k\pi}(E)$ the full t -matrix obtained from the solution of Eq. (2). It is easy to see that Eq. (7) corresponds to the following decomposition of the full $t_{\pi\pi}$ matrix

$$t_{\pi\pi}(E) = t_{\pi\pi}^B(E) + \sum_{n=1}^N t_{\pi\pi}^{R_n}(E), \quad (8)$$

where the new background operator is defined as $t_{\pi\pi}^B(E) = v_{\pi\pi}^B(E) + \sum_k v_{\pi k}^B(E) g_k(E) t_{k\pi}(E)$. We call this the "resonant background", because it contains resonance contributions via the full scattering matrix $t_{k\pi}(E)$.

It can be shown that the sum of the two terms on the r.h.s. of Eq. (7) can be expressed by a single term as represented by the diagram on the l.h.s. in Fig. 2, which consists of a bare initial $\pi N R_n$ vertex, followed by a dressed resonance propagator and then finally decay through a dressed $\pi N R_n$ vertex. Now it becomes obvious that $t_{\pi\pi}^{R_n}$ should have the standard Breit-Wigner form, $\sim (W - M_{R_n} + i\Gamma_{R_n}/2)^{-1}$, near the resonance position. The energy W where $\text{Re } t_{\pi\pi}^{R_n}$ crosses zero can be considered as the physical mass of the R_n resonance. The total width can be determined using the classical definition as the difference of energies where $\text{Im } t_{\pi\pi}^{R_n}(W) = \frac{1}{2} \text{Im } t_{\pi\pi}^{R_n}(M_R)$. Our final results for the resonance parameters are summarized in Table I.

It is seen that the above analysis of the elastic πN scattering indicates the existence of four S_{11} resonances. Now let us check this finding by an independent analysis of pion photoproduction using the dynamical model developed in Refs. [8,9,19] (hereafter called DMT (Dubna-Mainz-Taipei) model). We will again be brief about the DMT model and refer the readers to Ref. [9] for the details.

The essence of the dynamical model is to express the t -matrix for pion photoproduction as

$$t_{\gamma\pi}(E) = v_{\gamma\pi} + \sum_k v_{\gamma k} g_k(E) t_{k\pi}(E), \quad (9)$$

where $v_{\gamma k}$ is the transition potential for the $\gamma N \rightarrow kN$ reaction ($k = \pi$ or η), $t_{k\pi}$ is the full kN scattering t -matrix of Eq. (2), and g_k is the free kN propagator.

In the case where the transition potential $v_{\gamma\pi}$ consists of two terms,

$$v_{\gamma\pi}(E) = v_{\gamma\pi}^B + v_{\gamma\pi}^R(E), \quad (10)$$

where $v_{\gamma\pi}^B$ is the background transition potential and $v_{\gamma\pi}^R(E)$ the contribution of a bare resonance R, we may decompose the resulting t-matrix into two terms [8],

$$t_{\gamma\pi}(E) = t_{\gamma\pi}^B(E) + t_{\gamma\pi}^R(E), \quad (11)$$

where

$$t_{\gamma\pi}^B(E) = v_{\gamma\pi}^B + \sum_k v_{\gamma k}^B g_k(E) t_{k\pi}(E), \quad (12)$$

$$t_{\gamma\pi}^R(E) = v_{\gamma\pi}^R + \sum_k v_{\gamma k}^R g_k(E) t_{k\pi}(E). \quad (13)$$

In our numerical calculations we have neglected the contribution of the η channel in the intermediate states in Eq. (12), because this contribution is found to be much smaller than for the π channels. Note that all the processes which start with the excitation of the resonance by the bare γNR vertex are summed up in $t_{\gamma\pi}^R$. This is similar to our definition Eq. (7) of the resonance contribution for πN scattering. Using the decomposition of Eqs. (11-13) we can now extract the value of the bare γNR vertex. As in the case of pion scattering, the corresponding background $t_{\gamma\pi}^B$ is called "resonant background" since it contains the full pion scattering t-matrix. Note that in Ref. [21] the background is defined differently,

$$\tilde{t}_{\gamma\pi}^B(E) = v_{\gamma\pi}^B + v_{\gamma\pi}^B g_\pi(E) \tilde{t}_{\pi\pi}^B(E), \quad (14)$$

$$\tilde{t}_{\pi\pi}^B(E) = v_{\pi\pi}^B + v_{\pi\pi}^B g_\pi(E) \tilde{t}_{\pi\pi}^B(E). \quad (15)$$

This definition corresponds to the so-called nonresonant (smooth) background, because it contains none of the resonance contributions. The corresponding resonance term $\tilde{t}_{\gamma\pi}^R = t_{\gamma\pi} - \tilde{t}_{\gamma\pi}^B$ describes a resonance with a dressed γNR vertex.

It can be easily proved that the following relation holds between $t_{\gamma\pi}^R$ and $\tilde{t}_{\gamma\pi}^R$:

$$\tilde{t}_{\gamma\pi}^R(E) = t_{\gamma\pi}^R(E) + v_{\gamma\pi}^B g_\pi(E) \tilde{t}_{\pi\pi}^R(E), \quad (16)$$

where $\tilde{t}_{\pi\pi}^R(E) = t_{\pi\pi}(E) - \tilde{t}_{\pi\pi}^B(E)$ is the dressed resonance contribution in pion scattering. Graphically the relation (16) is illustrated in Fig. 3.

The background potential $v_{\gamma\pi}^B$ contains Born terms with an energy dependent mixing of pseudovector and pseudoscalar πNN coupling and t-channel vector meson exchanges [16]. The mixing parameters and coupling constants were determined from an analysis of the nonresonant multipoles. The standard physical multipoles in channel $\alpha = \{l, j, I\}$ can then be expressed as

$$\begin{aligned} t_{\gamma\pi}^{B,\alpha}(\text{DMT}) &= v_{\gamma\pi}^{B,\alpha}(q_E, k) - \frac{1}{\pi} \int_0^\infty \frac{q'^2 dq'}{\mathcal{M}(q')} \frac{F_{\pi\pi}^{(\alpha)}(q_E, q'; E) v_{\gamma\pi}^{B,\alpha}(q', k)}{E - E(q') + i\epsilon} \\ &= v_{\gamma\pi}^{B,\alpha}(q_E, k) (1 + i q_E F_{\pi\pi}^{(\alpha)}(q_E, q_E; E)) - \frac{P}{\pi} \int_0^\infty \frac{q'^2 dq'}{\mathcal{M}(q')} \frac{F_{\pi\pi}^{(\alpha)}(q_E, q'; E) v_{\gamma\pi}^{B,\alpha}(q', k)}{E - E_{\pi N}(q')}, \end{aligned} \quad (17)$$

where $F_{\pi\pi}^{(\alpha)}$ is the pion-scattering amplitude with on-shell value $F_{\pi\pi}^{(\alpha)}(q_E, q_E) = [\eta_\alpha \exp(2i\delta_\alpha) - 1]/2iq_E$, with δ_α the phase shift and η_α the inelasticity parameter, and $\mathcal{M}(q) = E_\pi(q)E_N(q)/E_{\pi N}(q)$ the relativistic pion-nucleon reduced mass. We mention in passing that the so-called "K-matrix" approximation, as in the case of MAID and many others models, neglects the principal value integral in Eq. (17), i.e., only on-shell pion rescattering is taken into account in the parametrization of the background. In this case off-shell rescattering associated with the principal value integral contribution is phenomenologically absorbed in the resonance parameters while in the DMT model it is considered as a part of the background. Therefore, the resonance parts in DMT and K-matrix approach are different: in the DMT model the resonance is described by the amplitude $t_{\gamma\pi}^R$ with a bare electromagnetic vertex and, as we will see below, in the models based on the K-matrix approximation, the resonance description is essentially given by $\tilde{t}_{\gamma\pi}^R$ with a dressed electromagnetic vertex.

Following Ref. [16], we assume a Breit-Wigner form for the resonance contribution $t_{\gamma\pi}^{R,\alpha}(W)$,

$$t_{\gamma\pi}^{R,\alpha}(W) = \bar{\mathcal{A}}_\alpha^R \frac{f_{\gamma R}(W)\Gamma_R M_R f_{\pi R}(W)}{M_R^2 - W^2 - iM_R\Gamma_R}, \quad (18)$$

where $f_{\pi R}$ is the usual Breit-Wigner factor describing the decay of a resonance R with total width $\Gamma_R(W)$ and physical mass M_R . The expressions for $f_{\gamma R}$, $f_{\pi R}$ and Γ_R are given in Ref. [16]. In the DMT model the electromagnetic form factor $\bar{\mathcal{A}}_\alpha^R$ describes the bare γNR vertex. This is a free parameter to be determined from the experimental data.

In Fig. 4 (upper panel) we see that the resonant background in the DMT model (dash-dotted curve) is very important, in particular for $W > 1450$ MeV where it becomes large and negative. This is in contrast to the prediction based on the K-matrix approximation (dashed curve). The difference comes mainly from the principal value integral contribution in Eq. (17). Such a background will thus require a much stronger resonance contribution in order to describe the results of the recent partial wave analysis of Ref. [22]. Consequently, the dynamical model predicts much larger values for the electromagnetic form factors (or helicity amplitudes $A_{1/2}$) than those obtained with the K-matrix approximation..

In order to estimate the new values for the resonance parameters, we will first fit $\text{Im } {}_p E_{0+}$ in the photon energy range $1075 < W < 2300$ MeV only, thereby assuming that $v_{\gamma\pi}^{R,\alpha} = \sum_{n=1}^4 v_{\gamma\pi}^{R_n,\alpha}$. The results of our fit are presented in Tables II-IV and Fig 4. We would like to stress that, since the DMT background is large and negative even at $W > 1770$ MeV, the best fit requires two new S_{11} resonances with masses 1810 MeV and 2053 MeV, in addition to the well known resonances $S_{11}(1535)$ and $S_{11}(1650)$. In fact the χ^2 of the fit improves from 64 to 3.7 by introducing these two additional resonances. This result clearly indicates that, in agreement with our previous findings for pion scattering, our pion photoproduction model calls for a low-lying third S_{11} resonance which may be one of the missing resonance predicted by quark models [11] and is also indicated in an analysis of eta photoproduction [23].

Our next important result concerns the value of the helicity amplitude for the first $S_{11}(1535)$ resonance. Here we expect to get more reliable information by analyzing the observables (differential cross sections, beam, target and recoil asymmetries) in the full energy range $1075 < W < 1770$ MeV, similar to the work of Ref. [24]. In other words, we have to perform a new partial wave analysis including the new background description. For this purpose the resonances in the higher partial waves have to be taken into account as well. The details of our fitting procedure are described in Ref. [24]. We only note that our analysis includes experimental data for $E_\gamma < 1200$ MeV. In the proton channel the corresponding data base contains 14880 data points. We fix the parameters for the third and fourth S_{11} resonances using the results for $\text{Im } {}_p E_{0+}$ as described above. Our final results are shown in Fig. 5 and summarized in Table V. In general they are consistent with the earlier results obtained directly from $\text{Im } {}_p E_{0+}$.

Our final value for the bare helicity amplitude of the first $S_{11}(1535)$ resonance is $A_{1/2}(\text{bare}) = 116 \pm 3 \times 10^{-3} \text{GeV}^{-1/2}$. In order to get the dressed value, we first have to determine the nonresonant background $\tilde{t}_{\gamma\pi}^{B\alpha}$, as given by Eq. (14). The result for this background, shown in Fig. 6 (left panel) by the dashed curve, is small near resonance position. The dressed value for the $A_{1/2}$ can be calculated directly from $\text{Im } {}_p E_{0+}^{(1/2)}$ using the relation [25]

$$A_{1/2} = \sqrt{\frac{2\pi M_R \Gamma_R q_R}{k_R m_N \beta_\pi}} \text{Im } {}_p E_{0+}^{(1/2)} C_{\pi N}, \quad (19)$$

where q_R and k_R are the pion and photon momentum, respectively, at $W = M_R = 1528$ MeV and $C_{\pi N} = -\sqrt{3}$ is an isospin factor. Subtracting the contribution of the other S_{11} resonances we obtain $\text{Im } {}_p E_{0+}^{(1/2)} = (3.93 - 0.14) \times 10^{-3}/m_{\pi+}$, where the last number is the contribution of the nonresonant background $\tilde{t}_{\gamma\pi}^{B\alpha}$, and $A_{1/2}(\text{dressed}) = 72 \pm 2 \times 10^{-3} \text{GeV}^{-1/2}$. Another separation of the resonance and background contributions can be obtained by use of the K-matrix approximation for pion rescattering. In this case ${}_p E_{0+}^{(1/2)} = (3.93 - 0.42) \times 10^{-3}/m_{\pi+}$ and the corresponding helicity amplitude $A_{1/2}(\text{K-matrix}) = 67 \pm 2 \times 10^{-3} \text{GeV}^{-1/2}$, which is very close to the dressed value obtained above.

As a last step, we extract the bare and dressed values for $A_{1/2}$ from eta photoproduction. The formalism for this reaction is similar to the pion photoproduction case, the only difference being that in the eta channel it is important to take account of the coupling to the pion channel. The resonant background $t_{\gamma\eta}^B$ can then be written as

$$t_{\gamma\eta}^B(E) = v_{\gamma\eta}^B + v_{\gamma\eta}^B g_\eta(E) t_{\eta\eta}(E) + v_{\gamma\pi}^B g_\pi(E) t_{\pi\eta}(E), \quad (20)$$

where $t_{\eta\eta}(E)$ and $t_{\pi\eta}(E)$ are the full t-matrices describing eta scattering and eta production by pions, respectively, as obtained by solving Eq. (2).

Our results for the resonant background in the ${}_p E_{0+}$ channel are shown in Fig. 6 (right panel) by the dash-dotted curve. We can see that this background is about 30% of the total amplitude (solid curves), and that it originates mainly

from the coupling to the pion channel. Using Eq. (19) (with the eta momentum for q_R , branching ratio $\beta_\eta = 0.5$, and $C_{\eta N} = -1$) we can now extract $A_{1/2}(\text{bare})$, $A_{1/2}(\text{dressed})$ and $A_{1/2}(\text{K-matrix})$. The final results and a comparison with the results obtained for the first S_{11} resonance in pion photoproduction are given in Table VI. In general the values of the helicity amplitudes derived from the two reactions are consistent within 10%. Note that our bare values are also close to the result obtained in Ref. [29] ($A_{1/2} = 102 \times 10^{-3} \text{GeV}^{-1/2}$) by solving of the coupled Bethe-Salpeter equations. However, our dressed value considerably differs from the results of Ref. [26] where $A_{1/2}(\text{dressed}) = 118 \times 10^{-3} \text{GeV}^{-1/2}$. This is mainly due to the different total width Γ_R , which is 191 MeV in Ref. [26] and 95 MeV in our model. For example using Eq. (19), we can easily obtain that $A_{1/2}(\text{dressed}) \simeq 118 \sqrt{95/191} = 83 (\times 10^{-3} \text{GeV}^{-1/2})$ which is close to our result.

We thus conclude that the large differences for the helicity amplitude of $S_{11}(1535)$ resonance appearing in different analyses, are mainly due to the differences for the total widths. From our coupled channel analysis of pion scattering and pion photoproduction reactions we obtain $\Gamma_R \simeq 100$ MeV. Note that values close to ours were also obtained within the Pit-ANL and KSU models [27]. It seems that in order to clarify the situation for the total width, a new analysis of eta photoproduction is required, especially with the additional background contributions appearing due to the coupling to the pion channel.

In summary, we have performed a self-consistent analysis of pion scattering and pion photoproduction within a coupled channels dynamical model. The results indicate the existence of a third and a fourth S_{11} resonance with the masses 1803 ± 7 and 2117 ± 64 MeV. In the case of the pion photoproduction, we obtain background contributions to the imaginary part of the S -wave multipole which differ considerably from the result based on the K-matrix approximation. Within the dynamical model these background contributions become large and negative in the region of the $S_{11}(1535)$ resonance. Due to this fact much larger resonance contributions are required in order to explain the results of the recent multipole analyses. For the first $S_{11}(1535)$ resonance we obtain as values of the bare and dressed electromagnetic helicity amplitudes: $A_{1/2}(\text{bare}) = 116 \pm 3 \times 10^{-3} \text{GeV}^{-1/2}$ and $A_{1/2}(\text{dressed}) = 72 \pm 2 \times 10^{-3} \text{GeV}^{-1/2}$. Similar values can be derived from eta photoproduction if one takes the same total width ($\Gamma_R = 95 \pm 5$ MeV) as in pion scattering and pion photoproduction.

ACKNOWLEDGMENTS

S.K. and L.T. are grateful to the Physics Department of the NTU for the hospitality extended to them during their visits. This work is supported in part by the National Science Council/ROC under grant NSC 90-2112-M002-032, by the Deutsche Forschungsgemeinschaft (SFB 443), and by a joint project NSC/DFG TAI-113/10/0.

* Permanent address: Laboratory of Theoretical Physics, JINR Dubna, 141980 Moscow region, Russia.

- [1] Particle Data Group, Euro. Phys. J. C **15** (2000) 1.
- [2] R.A. Arndt, I.I. Strakovsky, R.L. Workman, and M.M. Pavan, Phys. Rev. C **52** (1995) 2120.
- [3] G. Höhler, F. Kaiser, R. Koch, and E. Pietarinen, *Handbook of Pion-Nucleon Scattering*, [Physics Data No. 12-1 (1979)].
- [4] D.M. Manley and E.M. Saleski, Phys. Rev. D **45** (1992) 4002.
- [5] T. Feuster and U. Mosel, Phys. Rev. C **58** (1998) 457.
- [6] R.E. Cutkovsky, C.P. Forsyth, R.E. Hendrick, and R.L. Kelly, Phys. Rev. D **20** (1979) 2839.
- [7] C.T. Hung, S. N. Yang, and T.-S.H. Lee, J. Phys. G20 (1994) 1531; Phys. Rev. C64 (2001) 034309.
- [8] S. S. Kamalov and S. N. Yang, Phys. Rev. Lett. **83** (1999) 4494.
- [9] S. S. Kamalov, S. N. Yang, D. Drechsel, O. Hanstein, and L. Tiator, Phys. Rev. C **64** (2001) 032201(R).
- [10] S. S. Kamalov, G.-Y. Chen, S. N. Yang, D. Drechsel, and L. Tiator, Phys. Lett. B 522 (2001) 27.
- [11] M. M. Giannini, E. Santopinto, A. Vassallo, Nucl. Phys. A699 (2002) 308.
- [12] B. Saghai and Zhenping Li, nucl-th/0202007.
- [13] M. Cooper and B. Jennings, Nucl. Phys. A500 (1989) 553.
- [14] L. Tiator, C. Bennhold and S. S. Kamalov, Nucl. Phys. A580 (1994) 455.
- [15] B. C. Pearce and B. Jennings, Nucl. Phys. A528 (1991) 655.
- [16] D. Drechsel, O. Hanstein, S.S. Kamalov, and L. Tiator, Nucl. Phys. A645 (1999) 145.
- [17] A. I. L'vov, V. A. Petrun'kin and M. Schumacher, Phys. Rev. C55 (1997) 359.
- [18] T. P. Vrana, S. A. Dytman and T.-S. Lee, Phys. Rep. 328 (2000) 181.
- [19] S. N. Yang, J. Phys. G11 (1985) L205.

[20] R. A. Arndt, I. I. Strakovsky, R. L. Workman, and M. M. Pavan, Phys. Rev. C52 (1995) 2120
[21] T. Sato and T.-S.H. Lee, Phys. Rev. C 54 (1996) 2660.
[22] R. A. Arndt, W. J. Briscoe, I. I. Strakovsky, and R. L. Workman, nucl-th/0205067
[23] B. Saghai and Zhenping Li, nucl-th/0202007.
[24] S. S. Kamalov, D. Drechsel, L. Tiator, and S. N. Yang, N*2001 Workshop (s.a.) nucl-th/0106045.
[25] R. A. Arndt, R. L. Workman, Zh. Li, and L. D. Roper, Phys. Rev. C42 (1990) 1864
[26] W.T. Chiang, S.N. Yang, L. Tiator, and D. Drechsel, Nucl.Phys. A700 (2002) 429.
[27] Bennhold et al. Proceeding of N*2001 Workshop
[28] O. Hanstein, D. Drechsel, and L. Tiator, Nucl. Phys. A632 (1998) 561.
[29] C. Deutsch-Sauermann, B. Friman and W. Nörenberg, Phys. Lett. B409 (1997) 51.

Resonances	M_R^0	M_R	Γ_R
R_1	1559	1510	99
R_2	1721	1681	124
R_3	1810	1797	295
R_4	2159	2182	421

TABLE I. S_{11} resonance parameters obtained from πN scattering: M_R^0 and M_R are the bare and physical (dressed) masses, respectively; Γ_R is the total width.

Parameters	β_π	M_R	Γ_R	$A_{1/2}$
R_1	0.40	1523 ± 3	97 ± 13	110 ± 7
R_2	0.85	1688 ± 3	157 ± 14	130 ± 6

TABLE II. Estimation of the S_{11} resonance parameters obtained by fitting $\text{Im } {}_p E_{0+}$ in the energy range $145 \text{ MeV} < E_\gamma < 1200 \text{ MeV}$ or $1075 \text{ MeV} < W < 1900 \text{ MeV}$, with only two S_{11} resonances.

Parameters	β_π	M_R	Γ_R	$A_{1/2}$
R_1	0.40	1523 ± 3	97 ± 13	110 ± 7
R_2	0.85	1687 ± 2	152 ± 8	103 ± 5
R_3	0.50	1942 ± 12	561 ± 36	135 ± 7

TABLE III. Estimation of S_{11} resonance parameters obtained by fitting $\text{Im } {}_p E_{0+}$ in the energy range $145 \text{ MeV} < E_\gamma < 2000 \text{ MeV}$ or $1075 \text{ MeV} < W < 2300 \text{ MeV}$, with three S_{11} resonances ($\chi^2/95 = 4.8$). The parameters for the first S_{11} resonance were fixed according to Table I.

Parameters	β_π	M_R	Γ_R	$A_{1/2}$
R_1	0.40	1523 ± 3 (1524)	97 ± 13	110 ± 7
R_2	0.85	1673 ± 3 (1688)	118 ± 6	85 ± 9
R_3	0.50	1810 ± 12 (1861)	295 ± 11	118 ± 12
R_4	0.50	2053 ± 11 (2008)	267 ± 27	56 ± 8

TABLE IV. Estimation of the S_{11} resonance parameters obtained by fitting $\text{Im } {}_p E_{0+}$ in the energy range $145 \text{ MeV} < E_\gamma < 2000 \text{ MeV}$ or $1075 \text{ MeV} < W < 2300 \text{ MeV}$ with four S_{11} resonances ($\chi^2/95 = 3.7$). The parameters for the first S_{11} resonance were fixed according to Table I. In brackets: quark model predictions of Ref. [11] for the masses M_R .

Parameters	M_R	Γ_R	$A_{1/2}(\text{bare})$
R_1	1528 ± 1	95 ± 5	116 ± 3
R_2	1684 ± 1	112 ± 7	68 ± 2

TABLE V. Our final results for the resonance parameters of the first two S_{11} resonances obtained by fitting observables in the energy range $145 \text{ MeV} < E_\gamma < 1200 \text{ MeV}$ or $1075 \text{ MeV} < W < 1770 \text{ MeV}$. The parameters for the third and fourth S_{11} resonances were fixed with the values from Table IV. The branching ratios are $\beta_\pi = 0.4$ and 0.85 for R_1 and R_2 , respectively.

$A_{1/2}$	(γ, π)	(γ, η)
$A_{1/2}(\text{bare})$	$116 \pm 3 \quad (6.1)$	$108 \pm 4 \quad (17.8)$
$A_{1/2}(\text{dressed})$	$72 \pm 2 \quad (3.8)$	$81 \pm 3 \quad (13.5)$
$A_{1/2}(\text{K-matrix})$	$67 \pm 2 \quad (3.5)$	$83 \pm 3 \quad (13.8)$

TABLE VI. $A_{1/2}(\text{bare})$, $A_{1/2}(\text{dressed})$ and $A_{1/2}(\text{K-matrix})$ helicity amplitudes for the $S_{11}(1535)$ resonance obtained in pion and eta photoproduction using the coupled channel dynamical model (see text). The values correspond to $M_R = 1528 \text{ MeV}$, $\Gamma_R = 95 \text{ MeV}$, $\beta_\pi = 0.4$, and $\beta_\eta = 0.5$. In the brackets we give the imaginary part of the corresponding E_{0+} multipoles at the resonance position in units of $10^{-3}/m_{\pi+}$.

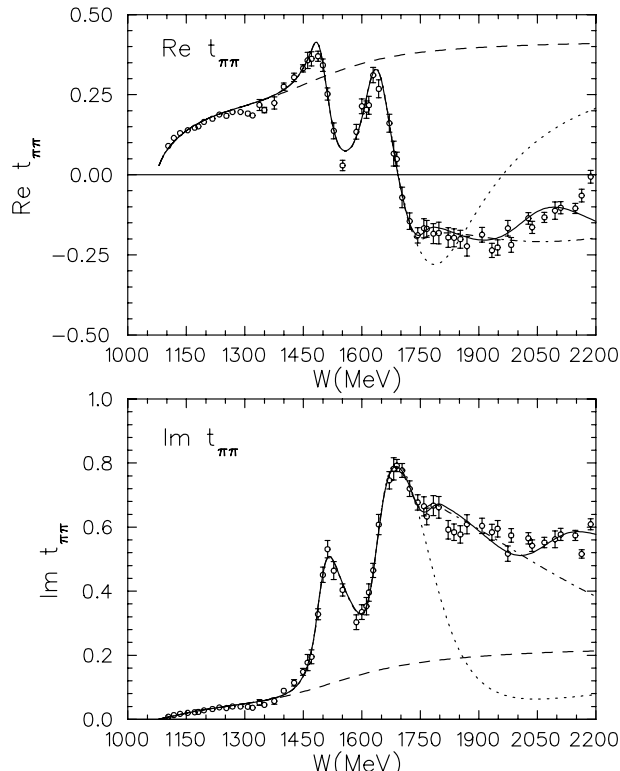


FIG. 1. Real and imaginary parts of the S_{11} pion scattering amplitude. Dashed curves: nonresonant background contribution $t_{\pi\pi}^B$. Dotted, dash-dotted and solid curves: total $t_{\pi\pi}$ amplitude obtained after the best fit with two, three and four S_{11} resonances, respectively. Data points: results of the single energy analysis from Ref. [20].

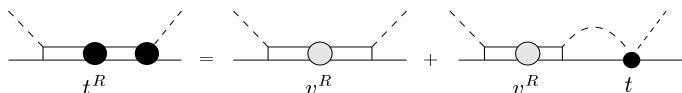


FIG. 2. Graphical representation of the resonance contribution to pion scattering as determined by Eq. (7). The grey circle in the resonance propagators denotes the presence of the width associated with the $\pi\pi N$ contribution, the black circle corresponds to the propagators with total width and physical mass.

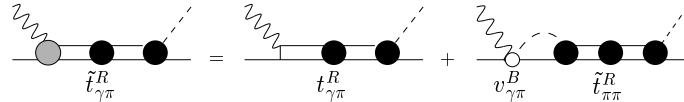


FIG. 3. Graphical representation of the resonances with dressed and bare electromagnetic vertices.

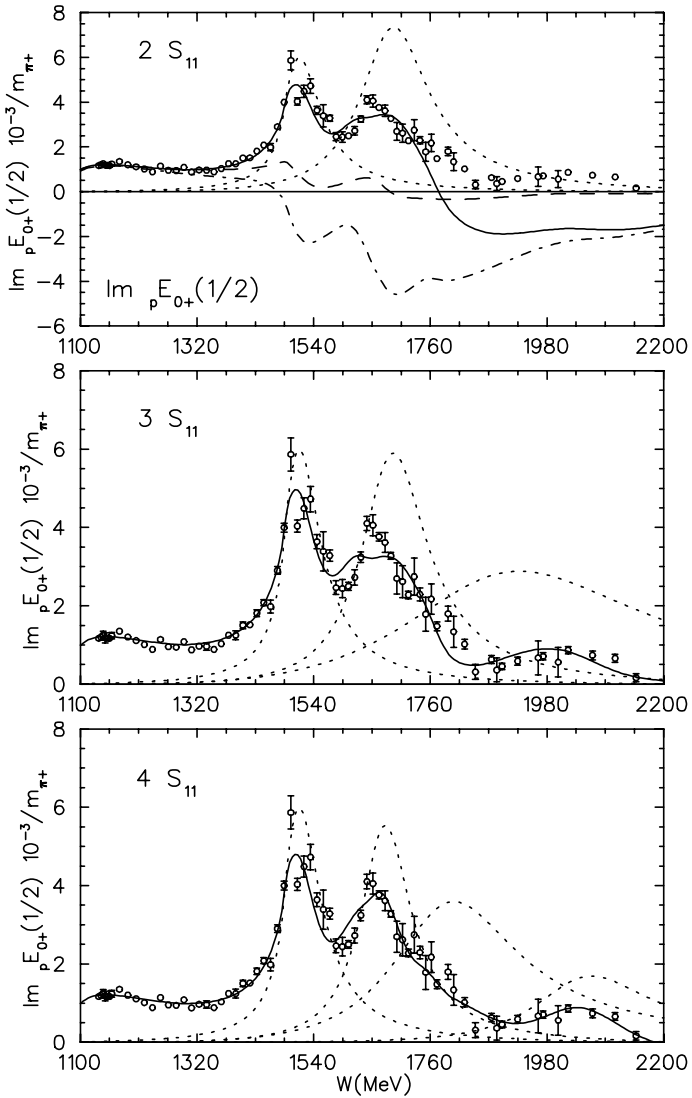


FIG. 4. Imaginary parts of the $pE_{0+}^{1/2}$ multipoles. Dashed and dash-dotted curves in the upper panel: background contributions obtained using K-matrix approximation and DMT model, respectively. Solid curves in the upper, middle and low panels: total multipole with two, three and four S_{11} resonances, respectively. The individual contributions from each resonance (with bare electromagnetic vertex) are shown by the dotted curves. The corresponding resonance parameters are given in Tables II-IV. Data points: results of the single energy multipole analysis from Ref. [22].

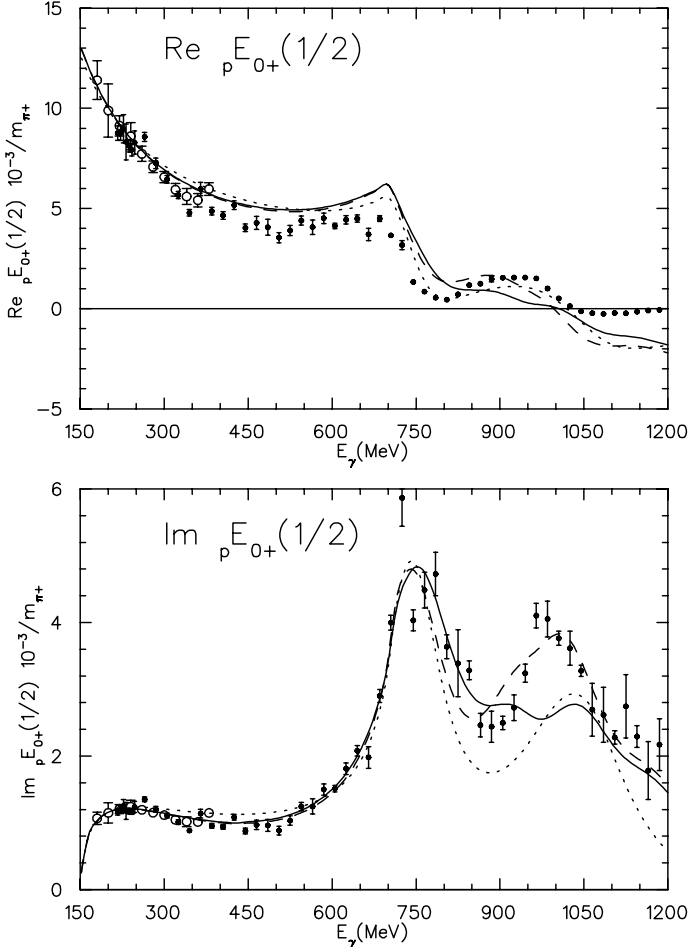


FIG. 5. Real and imaginary parts of the $p E_{0+}^{1/2}$ multipole. Dashed and solid curves: results obtained by fitting $\text{Im } p E_{0+}^{1/2}$ (see Table IV) and the observables (see Table V), respectively. Dotted curve: result of MAID2000 [16]. Data points: results of the single energy multipole analysis of Ref. [28] (○) and Ref. [22] (●).

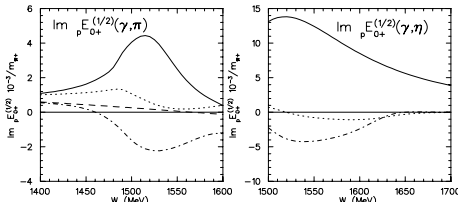


FIG. 6. Imaginary parts of the $p E_{0+}^{1/2}$ multipoles for pion (left figure) and eta (right figure) photoproduction on the proton. Dash-dotted and dashed curves are resonant, t^B (Eqs.(11-13)), and nonresonant, \tilde{t}^B (Eq.(14)), backgrounds, respectively. In the case of eta photoproduction the main contribution to the resonant background comes from the coupling to the $\pi\eta$ channel, the contribution of the nonresonant background vanishes. Dotted curves: background according to the K-matrix approximation. Solid curves: total result including contributions of $S_{11}(1535)$ resonance and background.